ELSEVIER

Journal of Neuroscience Methods 56 (1995) 125–131

JOURNAL OF NEUROSCIENCE METHODS

A multi-electrode array for combined microiontophoresis and multiple single-unit recordings

Sebastian Haidarliu [a,*], Daniel Shulz [b], Ehud Ahissar [a]

[a] *Department of Neurobiology, The Weizmann Institute of Science, Rehovot, Israel*
[b] *CNRS, Institute A. Fessard, 91198 Gif sur Yvette, France*

Received 28 February 1994; revised 24 June 1994; accepted 24 June 1994

Abstract

A remotely controlled multi-electrode array, equipped with a combined electrode (CE) and 3 regular tungsten-in-glass electrodes (TEs) is described. The CE enables ejection of different neuroactive substances from 6 barrels and recording of single-unit activity from the etched tungsten rod placed in the central glass capillary. The CE is prepared with standard tungsten rod, glass-capillaries, and regular micropipette pullers. Such CEs possess a good stiffness-flexibility balance, length, easy cell isolation, high stability of recordings, effective ejection properties, and ability to survive penetration of dura. The efficiency of a 4-electrode array, including the CE, was tested by recording the effects of extracellularly ejected drugs (glutamate, acetylcholine and atropine) on single neurons in the auditory cortex of anesthetized guinea pigs. Induced modifications of single-neuron firing patterns and evoked responses were in agreement with the known effects of individual and combined applications of these drugs. Using this multi-electrode array and spike sorting techniques, the pharmacological environment of up to 12 simultaneously recorded cells can be modulated, and its effect on single neurons and on their interactions can be monitored at distances of up to 900 μm from the CE's tip.

Keywords: Multi-electrode array; Combined electrode; Microiontophoresis; Multiple single-unit recording; Auditory cortex; Neuromodulator; Spike sorting; Cross-correlation

1. Introduction

Specific functional properties of sensory cortical neurons can be modified during a critical period of postnatal development and during particular phases of learning in the adult (review in Frégnac and Shulz, 1993). Recently, it has been shown that the plasticity of functional connectivity between pairs of neurons in the auditory cortex of adult awake monkeys depends on the behavioral state of the animal (Ahissar et al., 1992). The involvement of neuromodulatory systems in associative learning has been proposed on the basis of a large number of physiological and behavioral data (review in Aston-Jones, 1985). However, the underlying pharmacology, as well as the precise nature of the information carried by these factors, are still conjectural. In order to investigate the potential role of different neuromodulators in the plasticity of functional connectivity of local cortical circuits, we developed a multi-electrode array for combined microiontophoresis and multiple single-unit recordings.

Most of the electrodes designed for both microiontophoresis and extracellular recordings and described in the literature are not suited for multiple recordings in deep brain regions or cortical areas distanced from the location of penetration (e.g., the primary auditory cortex in rhesus monkeys). Glass multi-barreled electrodes for combined iontophoresis and neural activity recording are currently used (review in Stone, 1985). However, they suffer from noise coupling when passing current through the drug barrels while recording through the central barrel; they are too fragile to penetrate through the dura without damage; they allow the recording of a single neuron at a time; and finally, a compromise between the optimal diameter for drug ejection and recording is difficult to achieve. One pos-

* Corresponding author. Tel.: (972) 8-343748; Fax: (972) 8-344140.

SSDI 0165-0270(94)00114-6

sibility to overcome these problems is to use a combination of a metallic recording electrode with a set of iontophoresis barrels (review in Millar, 1992). One method requires the gluing of prefabricated components (Gottschaldt et al., 1986; Godwin, 1993) which, however, usually renders an electrode with the length of the shaft too short for recording in deep brain structures or it includes too many preliminary steps in electrode fabrication (Perrett and Rolls, 1985). An alternative method is the manufacturing of a combined electrode (CE) in which the central barrel of the multi-barreled blank is filled with an etched tungsten rod, and the entire electrode is fabricated in a 1-step pulling (Hellier et al., 1990; Li et al., 1990). The electrodes thus obtained did not appear to be suitable for our purposes since they were too short (1.5–5 cm long) their diameter was at least 1 mm at 3 cm from the tip, and they were designed for single-electrode setup.

We describe here a method for producing a combined metal-cored multi-barreled electrode with a 9-cm-long shaft and a diameter of 0.6 mm at 7 cm from the tip. This CE is suitable for recordings of several units in deep regions of the brain and, when assembled with 3 additional TEs and connected to 4 spike sorters (see Methods), the entire setup allows the recording of up to 12 units simultaneously, and the modulation of the pharmacological environment of the recorded cells.

2. Methods

2.1. Preparation of the CE

The CE was constructed from a tungsten rod (125 μm in diameter, Frederick Haer, Brunswick, USA) and 7 glass capillary blanks (Borosilicate glass; outer diameter: 1.2 mm; inner diameter: 0.69 mm; length: 10 cm) with omega dot fiber for rapid filling (Clark Electromedical Instruments, UK). At one end of the tungsten rod, a 6-mm portion was etched in the following solution: 71 g $NaNO_2$, 34 g KOH in 100 ml of distilled water (Levick, 1972) to obtain a conical shape, nearly 1 μm diameter at the tip and about 4 μm at 25 μm from the tip. The duration of the electrolytic etching with an AC power supply at 8 V was 5 ± 1 min. After etching, the tungsten rod was back fed into the central capillary of a bundle of 7 capillaries.

The capillaries were fastened together at their ends by two pieces of heat-shrink tubing (inner diameter: 4.5 mm; length: ~ 1 cm) (Fig. 1A). The shrink tubing also protected capillaries from breaking when they were grasped in the puller chucks for pulling. The pipette blank was pulled down by a microelectrode vertical puller (PE-2, Narishige, Japan). The upper chuck of the puller was replaced by a chuck that had a hole in its center in order to allow the etched end of the

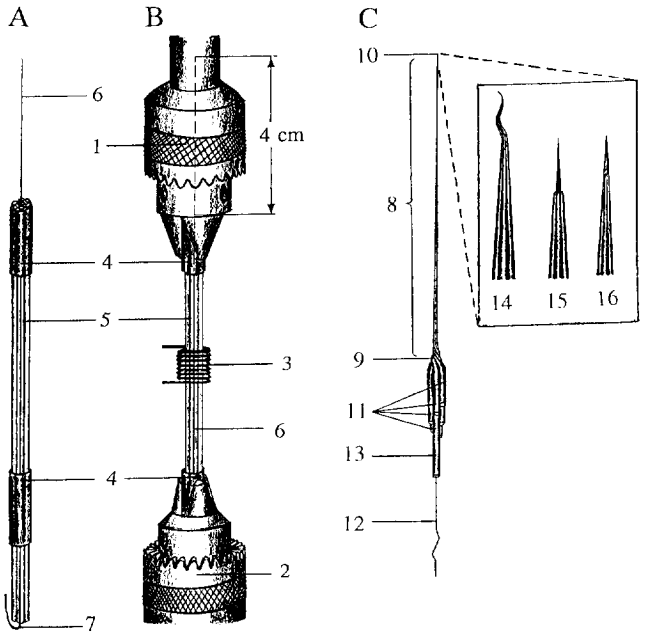

Fig. 1. A capillary blank (A), its positioning in the vertical puller (B) and a CE (C). A: the etched tungsten rod (6) is back-fed into the central barrel of the capillary bundle (5) fastened by heat-shrink tubings (4). The lower end of the rod is bent (7) to prevent it from moving while twisting the blank. B: the blank is held in a PE-2 vertical puller by two drill chucks (1 and 2). The distance between the heating coil (3) and the tip of the tungsten rod will determine the length of the electrode shaft (C, 8). To increase this length, a hole was made in the upper chuck (1) allowing the tungsten rod to protrude 4 cm from the capillaries. C: the main characteristic of this electrode is the length of its shaft (8–9 cm) between the twisting point (9) and the tip (10). The glass capillaries were cut at different levels to avoid cross-contamination when filling them (11). Since the tungsten rod (12) is used for both mechanical and electrical connections, the central glass capillary (13) is longer, and a drop of glue is used to fix the metallic rod in the glass, solidifying the connections. Inset: possible CE tip shapes after pulling. Two main parameters affected the shape of the tip during pulling, the coil temperature and the timing of the magnet activation. Too high temperature and delayed activation of the magnet produced a long glass whisker at the tip (14). On the other hand, too low temperature or too early activation of the magnet caused the capillaries to break, and the exposed tungsten rod was generally too long (15). Under optimal conditions, a good tip profile could be obtained (16).

tungsten rod to protrude by about 4 cm (Fig. 1B). The distance between the middle of the heating coil and the tip of tungsten rod determined the length of the electrode shaft (Fig. 1C).

The fabrication of the CE was performed in 2 stages: twisting and pulling. For twisting, the pipette blank was placed in the center of a heater coil, the upper loop of which was 35 mm down from the butt end of the upper chuck. The heater coil consisted of a nichrome wire, 1 mm in diameter that contained 8 turns. The inner diameter of this coil was 7 mm and its height 14 mm. When the current was switched on (at 14.5 A), a heated portion of the glass bundle melted, and the

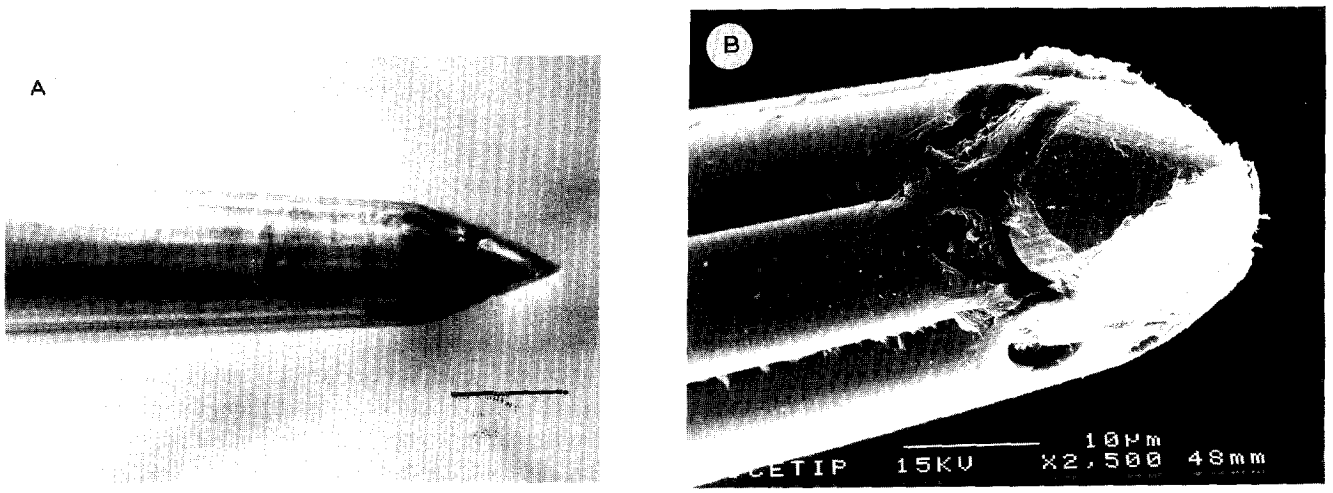

Fig. 2. Micrographs of the tips of 2 CEs after grinding. A: photomicrograph demonstrating a conical shape of the exposed by grinding tungsten tip which is stiff and permits an easy penetration into brain tissue. Scale bar: 20 μm. B: scanning electron micrograph of a CE tip demonstrating the shape of the ground tungsten rod and iontophoretic barrels which are uniformly distributed around the tungsten tip.

lower chuck was rotated slowly by hand for about 180°, while a small pull (1–2 mm) was allowed to the glass.

After the bundle cooled, the heat was switched on again, and proper pulling was performed. In contrast with the method proposed by Li et al. (1990) who cancelled the operation of all the Narishige automatic switches, we disabled only the switch of the heating coil. The other two were adjusted so that one would

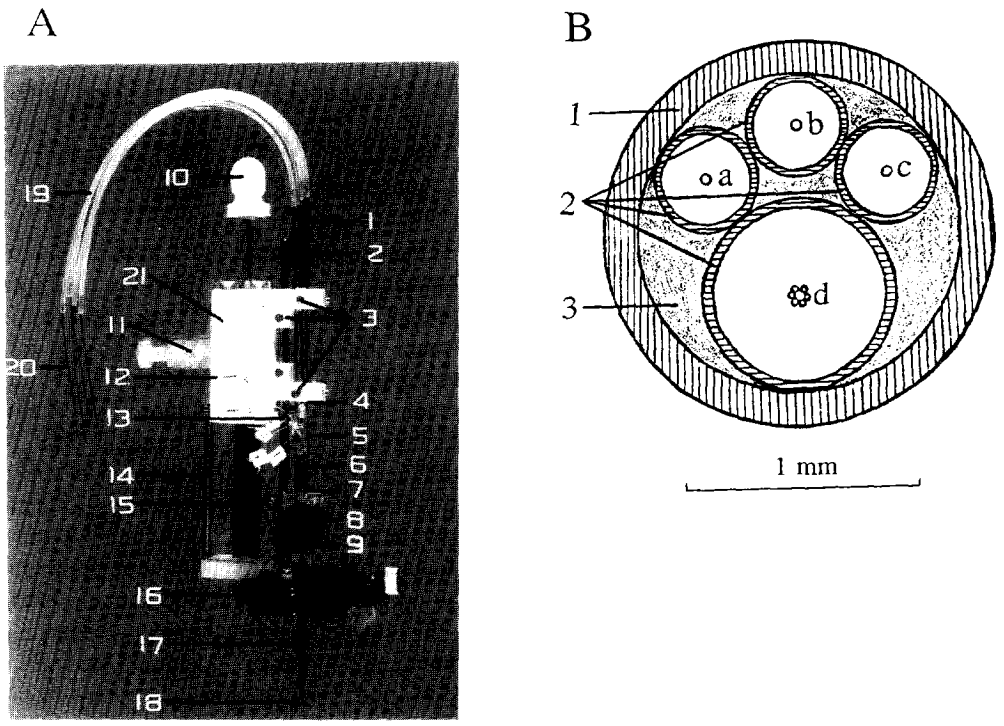

Fig. 3. Microdriving terminal. A_1: distal guiding and fixating tube; A_2: stainless steel height adjusting bar; A_3, fixation screws; A_4: electrode fixation tube; A_5: regular TE electrode; A_6: CE; A_7: polyimide tubing for regular electrode; A_8: plexiglass guiding box; A_9: polyimide tubing for combined electrode; A_{10}: *Z* direction adjustment knob; A_{11}: screw clamp for iontophoresis control cable; A_{12}: male amphenol pin; A_{13}: teflon-insulated silver wire; A_{14}: spring; A_{15}: brass guide rail; A_{16}: *X,Y*-manipulating table; A_{17}: stainless steel guide tube; A_{18}: bevelled end of the stainless steel guide tube; A_{19}: teflon tubing; A_{20}: advancing flexible shaft. These shafts are connected to de Ribaupierre's drive system; A_{21}: teflon fixture. B: schematic cross-section of the stainless steel guide tube (17). B_1: the wall of the stainless steel guide tube; B_2: the walls of the polyimide tubings; B_3: intertubing space filled with superglue; B_{a-d}: the projections of the electrodes' tips. Approximate horizontal distances between the tips are: a–b and b–c, 400 μm each; a–c, 630 μm; d–a and d–c, 600 μm each; d–b, 720 μm.

activate the magnet when the etched tip of the tungsten rod crossed the central point of the heating coil, and the other would terminate all controlled operations when the electrode's tip emerged from the heating coil.

The coil temperature and the timing of magnet activation were crucial for proper tip forming. The best tip shape was obtained when the coil was powered by 14–15 A of current. If the coil temperature was too high tips with a long, thick whisker were usually obtained; if the temperature was too low, glass capillaries often broke before the tip was covered with glass. Under optimal conditions, capillaries for iontophoresis can be made that are very thin and finish together or within 5 μm of the tip of the tungsten rod (Fig. 1C, inset). The diameter of such capillaries 50 μm from their tip is 1–2 μm and these CEs were easily ground with a microgrinder EG-3 (Narishige, Japan) under a binocular microscope. The configuration of the exposed portion of the tungsten rod was determined according with the angle of the electrode, the pressure, and the grinding duration. Usually, a conical tungsten tip was formed of 10–25 μm and the diameter at the base of the exposed tungsten was 10–20 μm (Fig. 2A). The impedance (at 1 kHz) of the ground electrode measured with its tip fully immersed in saline, ranged from 0.2 to 0.6 MΩ. The overall diameter of the tungsten and the glass pipettes near the exposed tip was 15–25 μm. Usually, the capillaries near the tip were stretched around the tungsten rod, resulting in oval shape of the capillary orifices which are well seen in scanning electron micrograph (Fig. 2B). The long orifice diameter was usually between 3 and 6 μm, and the short one from 1 to 3 μm. Such capillary shape and dimensions result in rapid and easy filling which is not accompanied with liquid penetration in empty neighboring barrels.

2.2. Filling of iontophoretic pipettes

To reduce cross-contamination when filling the iontophoretic pipettes a staggered arrangement of the pipettes was obtained by cutting the capillaries with a diamond file 10–20 mm from the twisting point. This provided about 2 mm between the orifices of neighboring capillaries (numbered 1–6, Fig. 1C). Filling with different solutions was accomplished with syringes equipped with plastic pipette tips that had been pulled to obtain long thin tubings at their end, which were each inserted into the separate capillaries up to the twisting point. The impedance of the iontophoretic barrels ranged from 20 to 80 MΩ depending on the filling solution and the diameter of capillary orifice. The whole filling procedure was made under microscopic inspection.

2.3. Assembling of the multi-electrode microdrive system

This system is composed of a microdriving terminal (Fig. 3), developed originally by M. Abeles and E. Vaadia at The Hebrew University, Jerusalem, and a compact remotely controlled microelectrode drive system allowing to advance and measure independently the position of 4 microelectrodes, designed by Y. de Ribaupierre and built at the Institute of Physiology, University of Lausanne (7 rue du Bugnon, CH-1005 Lausanne, Switzerland). The latest includes also 4 head-stage amplifiers, one for each electrode. The outputs of the head-stage amplifiers were connected to a multi-channel amplifying and filtering system (MCP 8000, Alpha-Omega Engineering, PO Box 2091, Nazareth, Israel).

After the capillaries were filled with different solutions the CE was introduced into 1 of the 4 polyimide tubing fixed inside a stainless steel guide (16-ga needle) of the microdriving terminal (Fig. 3B), and a teflon-insulated silver wire (diameter: 125 μm) was introduced into each of the 6 capillaries. These wires connected the capillaries to a Neurophore-BH-2-microiontophoresis system (Medical System, USA). Three tungsten-in-glass electrodes (TEs) were back fed into the other 3 polyimide tubings. Mechanical and electrical connections were established for each of the electrodes, and the orifice of each capillary was covered with vaseline to avoid evaporation of the liquid.

3. Performance test

Pilot experiments were performed on the auditory cortex of anesthetized (urethane, 1.2 g/kg, i.p., supplemented by ketalar, 20–25 mg/kg, i.m.) Dunkin-Hartley guinea pigs (*Cavia porcellus Linnaeus*), whose heads were rigidly fixed in a special holder that provided free access for acoustic stimuli. The 6-cm-long stainless steel guide, with the CE and 3 TEs, was brought as close as possible to the dura over the auditory cortex (in a first series of experiments the dura was removed) using a binocular microscope, and the 'zero' position for each of the electrodes was determined. After this, the movement of each electrode and drug ejection were remotely controlled. Once the neuronal activities appeared, 4 spike sorters (MSD-2, Alpha-Omega, Nazareth, Israel) were used to isolate single- and multi-unit spikes for each of the 4 electrodes. Signal-to-noise ratios for well isolated cells were usually in the range of 5–20. Iontophoretic applications, in general, did not significantly affected noise levels, spike shapes or spike amplitudes.

This method, based on wave form recognition, allowed the isolation of up to 12 different units. Like for other methods, based on amplitude discrimination or

cluster separation in a parametric space, particular care has to be taken during the initial phase of template determination to detect the spikes of single units even when they are changed in shape or amplitude during, for example, bursting activity or iontophoretic application. Spontaneous neuronal activity, responses to acoustic stimuli, and responses to iontophoretic drug administrations were studied.

Isolated single units were usually stable for several hours. Fig. 4 shows an example of a 2.5-h continuous recording, during which the shapes of the spikes of simultaneously recorded units were essentially unchanged. It should be noted, that the electrodes' tips in this setup were optimized for stability in the expense of isolation. Sharper tips, for example, would usually result in a better isolation and worse stability. In some instances, spike shapes were not totally stable throughout the long recording periods. Thus, cell isolation was carefully inspected in real time, both through the MSD information (see Fig. 4) and the oscilloscopic monitoring of the original trace and delayed trace, on which detected spikes were marked. Whenever a deviation from the steady state was noticed, steps to correct it were taken, including threshold changes and template updating. In extreme cases, the electrode was moved a few micrometers to restore the original recording situation. If this could not be achieved, the cell recording was stopped.

Application of glutamate often excited 'nearby' cells, recorded from the CE, but only rarely affected 'distant' cells, recorded simultaneously from a TE. An example of the effect of glutamate on a nearby cell and a distant cell is depicted in Fig. 5A. The nearby neuron was immediately (within 0.4 s) and strongly excited by glutamate, while the distant neuron, recorded about 900 μm from the CE tip, was much less excited and exhib-

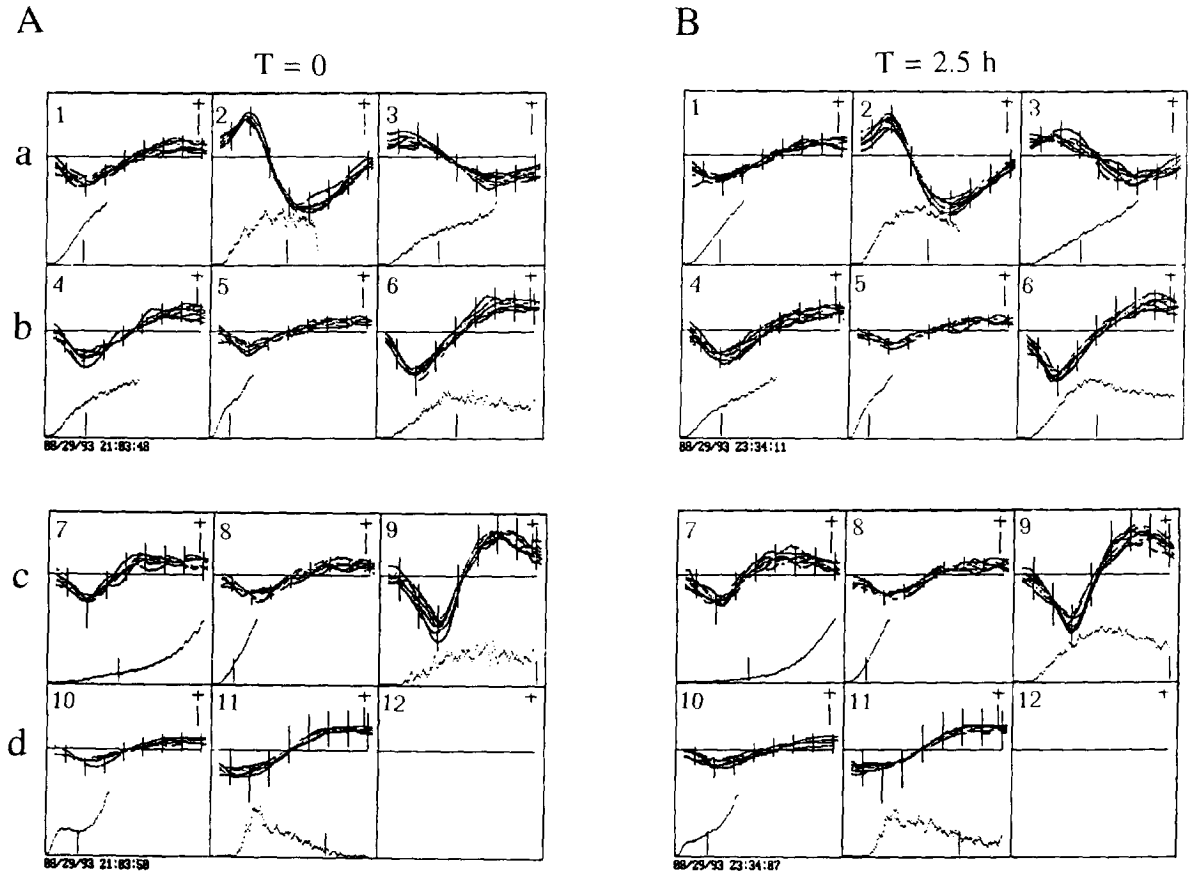

Fig. 4. Spikes recorded simultaneously by 3 TE (TE_a, units 1–3; TE_b, units 4–6; TE_c, units 7–9) and 1 CE (CE_d, units 10 and 11), at the beginning (A) and end (B) of a 2.5-h interval. Each small rectangle includes 8 superimposed spike shapes recorded from the same unit (top, abscissa: 0.6 ms full scale, ordinate: 150 μV half scale) and a histogram of accumulated 'Diff' values (bottom). Diff is an arbitrary parameter representing the root-mean-square difference between the recorded signal at a given time and the template. The vertical bar on the histogram denotes the threshold for spike detection; all signals with Diff less than the threshold were declared as spikes. The different windows were continuously graded according to the quality of spike isolation, and categorized as including 'single units' (i.e., 2, 6, 9, 11), 'contaminated single units' (i.e., 1, 3, 4, 7, 10), or 'multi-units' (i.e., 5, 8).

ited a longer latency (more than 1.6 s). To test the effect of glutamate on the neurons' firing patterns and interactions, the autocorrelation histograms (ACHs) of both cells and their cross-correlation histogram (CCH) were computed during glutamate application periods and inter-application, 'spontaneous', periods (Fig. 5B). No qualitative differences were observed using time resolution of 10 ms/bin. However, the increased firing rates emphasized the weak correlated activity at short delays (Fig. 5B, lower row, central peak).

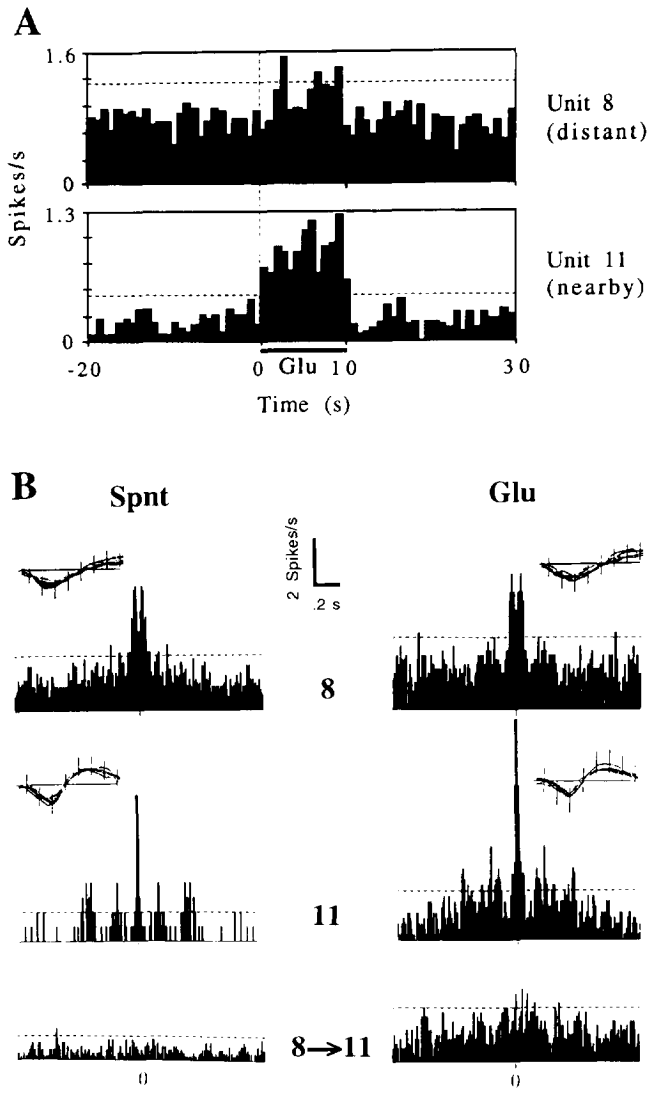

Fig. 5. The effects of glutamate application on nearby and distant cells. A: average cell responses to 40 applications of glutamate (−90 nA, 10 s) through the CE are presented. The 2 cells were recorded simultaneously from the CE (nearby) and a TE (distant) respectively, whose tips were separated by approximately 0.6 mm horizontally and 0.4 mm vertically. Automatic current compensation was used through an NaCl (3 M) filled barrel of the CE to avoid current effects. Bin size: 800 ms. Horizontal dashed lines: upper significance limits ($P < 0.005$), indicating the level of which 0.5% of equivalent Poisson processes would have higher values in a single bin. B: firing patterns of the same nearby and distant cells and their interaction. Upper row: ACH of the distant cell (#8). Middle row: ACH of the nearby cell (#11). Lower row: CCH of the 2 neurons. All histograms were calculated from a period containing 40 applications of glutamate (10 s on, 20 s off). Left column: histograms were calculated from the 'off' periods (total time: 608 s). Right column: histograms were calculated from the 'on' periods (total time: 400 s). Span: ±1 s; bin size: 10 ms. Horizontal dashed lines: upper significance limits ($P < 0.005$), as in A. Samples of the spike shapes in each condition are represented in the insets of the corresponding correlograms.

The relatively short latency of the distant cell activation may suggest that this activation was neuronal, rather than diffusional, in nature. Furthermore, immediate recovery of baseline firing rate at the end of glutamate application indicates that at least the late component of the response is mediated through activity of cortical network. However, we have preliminary evidence indicating that at least acetylcholine, carbachol and atropine are able to diffuse between neighboring electrodes. First, acetylcholine and carbachol often significantly ($P < 0.005$) affected the activity of distant cells. Second, we prepared a setup in which one of the TEs (electrode 4) was replaced by a second CE. When applications of acetylcholine or carbachol affected nearby cell's activity, we tried to block these effects using both local and distant applications of atropine. The pattern of blockade was similar in both conditions, although higher doses were required for the distant applications.

4. Discussion

The described multi-electrode array is suitable for combined microiontophoresis and multiple single-unit recordings. The length of this array makes it suitable for investigation of deep brain regions of various animals, including behaving monkeys. The required CE can be prepared using standard tungsten rods, glass capillaries, and standard equipment for pulling micropipettes. Such CEs have a stiffness-flexibility balance sufficient for reliable processing in multi-electrode microdriving terminal designed for remotely controlled microelectrode drive systems. Several CEs can be combined with several TEs to compose a multi-electrode setup for studying pharmacological effects on local cortical processing. The degree of control one has over the pharmacological environment of the recorded cells is determined by the number of CEs used, and their spatial arrangement: the more CEs, the better the control. On the other hand, a CE requires more space than a TE within the stainless steel guide, resulting in longer inter-electrode distances (Fig. 3B).

One of the aims of this study was to examine the spatial extent of the iontophoretic application. Using a setup of 1 CE and 3 TEs, we have demonstrated that distant cells can be affected by iontophoresis. Our preliminary results show that more than 30% of the distant cells (distanced up to 0.9 mm from the CE) can

be affected by acetylcholine or carbachol application (data not shown). However, more rigorous study is required to characterize the nature of these effects, and to examine the exact direct and/or indirect mechanism of such a distant iontophoretic influence.

Acknowledgements

We wish to thank J. Champagnat, Y. Frégnac and M. Segal for helpful comments on this manuscript. We are also grateful to S. Cohen, E. Gamzu and S. Serulnik for their assistance in the experiments, and to E. Klein for her skillful preparation of the scanning electron micrographs. D. Shulz was financed during his visit to Israel by the MDRI of the CNRS. This work was supported in part by The National Institute for Psychobiology in Israel (Grant 2-93RS), by The Israel Science Foundation administered by The Israel Academy of Sciences and Humanities, and by The Center for Absorption in Science, Ministry of Absorption, Israel.

References

Ahissar, E., Vaadia, E., Ahissar, M., Bergman, H., Arieli, A. and Abeles, M. (1992) Dependence of cortical plasticity on correlated activity of single neurons and on behavioral context. Science, 257: 1412–1415.

Aston-Jones, G. (1985) Behavioral functions of locus coeruleus derived from cellular attributes. Physiol. Psychol., 13: 118–126.

Frégnac, Y. and Shulz, D. (1993) Models of synaptic plasticity and cellular learning in mammalian visual cortex. In: V. Casagrande and P. Ahinkman (Eds.), Advances in Neural and Behavioral Development, Neural Ablex Publ., pp. 149–235.

Godwin, D.W. (1993) A tungsten-in-glass iontophoresis assembly for studying input-output relationships in central neurons. J. Neurosci. Methods, 49: 211–223.

Gottschaldt, K.-M., Hicks, T.P. and Vahle-Hinz, C. (1986) A combined recording and microelectrophoresis technique for input-output analysis of single neurons in the mammalian CNS.J. Neurosci. Methods, 23: 233–239.

Hellier, M., Boers, P. and Lambert, G.A. (1990) Fabrication of a metal-cored multi-barreled microiontophoresis assembly. J. Neurosci. Methods, 32: 55–61.

Levick, W.R. (1972) Another tungsten microelectrode. Med. Biol. Eng., 10: 510–515.

Li, B.-M., Mei, Z.-T. and Kubota, K. (1990) Multibarreled glass-coated tungsten microelectrode for both neuronal activity recording and iontophoresis in monkeys. Neurosci. Res., 8: 214–219.

Millar, J. (1992) Extracellular single and multiple unit recording with microelectrodes. In: J.A. Stamford (Ed.), Monitoring Neuronal Activity: A Practical Approach, IRL Press, Oxford, pp. 1–27.

Perrett, D.I. and Rolls, E.T. (1985) A technique for microiontophoretic study of single neurones in the behaving monkey. J. Neurosci. Methods, 12: 289–295.

Stone, T.W. (1985) Microiontophoresis and Pressure Ejection. IBRO Handbook Series: Methods in the Neurosciences, Vol. 8, J. Wiley.